Microwave response of hole and patch arrays

Melita C. Taylor, James D. Edmunds, Euan Hendry, Alastair P. Hibbins, and J. Roy Sambles
Electromagnetic Materials Group, School of Physics, University of Exeter, Stocker Road, Exeter EX4 4QL, United Kingdom
(Received 22 February 2010; revised manuscript received 8 July 2010; published 5 October 2010)

The electromagnetic response of two-dimensional square arrays of perfectly conducting square patches, and their complementary structures, is modeled utilizing a modal matching technique and employing Babinet's principle. This method allows for the introduction of progressively higher diffracted orders and waveguide modes to be included in the calculation, hence aiding understanding of the underlying causal mechanism for the observed response. At frequencies close to, but below, the onset of diffraction, a near-complete reflection condition is predicted, even for low filling fractions: conversely, for high filling fractions a near-complete transmission condition results. These resonance phenomena are associated with evanescent diffraction, which is sufficiently strong to reverse the step change in transmission upon establishment of electrical continuity; i.e., the connected structure demonstrates increased transmission with increasing filling fraction.

DOI: 10.1103/PhysRevB.82.155105 PACS number(s): 42.25.Bs, 41.20.Jb, 78.66.Bz, 42.25.Fx

The response of periodic metallic media to electromagnetic (EM) radiation has long been of interest to scientists across many diverse fields. For example, the topical field of study of surface plasmonics is often considered to have begun with the seminal result of Wood's in 1902, when he observed anomalous reflection bands from metallic gratings in the optical domain.[1] Thin structured metal films are of interest as they act as frequency selective surfaces (FSSs) (Refs. 2 and 3) and have numerous applications including shields for metallic radomes,[4] optical beam splitters,[5] and electromagnetic screening in medical and military applications.[6] Regular arrays of square patches and their inverse structures have been shown to act as low and high pass frequency filters, respectively.[7]

Standing EM surface waves established because of the periodicity of structured films result in band gaps at certain frequencies,[8,9] in analogy to the electron band gaps in semiconductors. According to Munk,[3] work on periodic photonic surfaces occurred as early as 1919. However, the seminal result with regards to the microwave regime is generally considered to have occurred in 1967 when extraordinary transmission through periodically arrayed holes was observed by Ulrich.[7] In the wider scientific community this phenomenon was not generally appreciated until 1998 when Ebbesen *et al.*[2] observed that subwavelength holes in thin metal screens provided enhanced optical transmission at frequencies near to the onset of diffraction.

The EM response of these and similar structures have been modeled in various ways, including transmission line models,[7,10,11] finite-element model (FEM) methods[12] as well as modal-matching methods[9,13–17] to name but a few. To gain an understanding of the physics underlying the observed responses an analytical modal matching method similar to that presented by McPhedran,[18] later adapted by Hendry *et al.*,[16] has been employed here. This method differs from some other methods[9,14,15] in that it includes the contributions from multiple-order waveguide modes, diffracted evanescent waves, and finite depth holes in the calculation[16] and is more similar to the approach used by Mary *et al.*[19] Another important difference between this and some of the other analytical models[9,14,17,20] is that this approach does not involve describing the system in terms of effective material parameters. The system investigated comprises a two-dimensional (2D) square array of square holes in a sheet of perfect electrical conductor (PEC) (structure A*) and its complementary system (structure A) [Fig. 1(a)]. A full and detailed analysis of structure A is unnecessary due to Babinet's principle.[21] Babinet's principle states that the sum of the transmission through an infinitely thin perforated screen, with the transmission through the complementary structure rotated by 90° about the normal to its plane, is equal to unity. (It is worth noting that, in the context of the present work, this is equivalent to a rotation of the incident polarization with no rotation of the structures.) The study of complementary structures by application of Babinet's principle has numerous precedents.[1,7,22–25] For finite thickness systems Babinet's principle is no longer exact, nevertheless it can still be used to guide our understanding.[26]

In the calculation of the transmission and reflection through the sample there are three distinct regions of space to

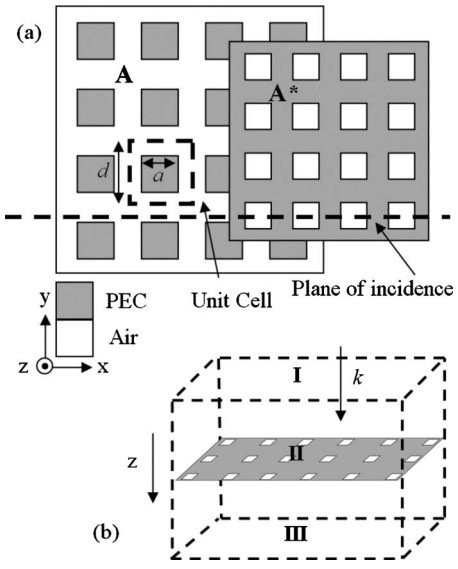

FIG. 1. Schematic showing: (a) investigated system; structure A and its complementary system A*; (b) defined regions (I–III) of the system used by the modal matching method.

be considered. These are the semi-infinite vacuum regions above (region I) and below (region III) the film, and the composite film itself (region II) [Fig. 1(b)]. Considering the hole array (structure A*) initially, the electric fields in the vacuum regions above and below the film can be described by a two-dimensional Fourier-Floquet expansion of the diffracted orders, [Eqs. (1)–(4)]. Note that the time-dependent field component, $\exp(i\omega t)$, has been omitted throughout for simplicity,

$$E_x^I = \sum_{m,n} A_x^{m,n} \psi_1^{m,n}(x,y)\exp(-ik_z^{m,n}z), \tag{1}$$

$$E_y^I = \sum_{m,n} A_y^{m,n} \psi_1^{m,n}(x,y)\exp(-ik_z^{m,n}z), \tag{2}$$

$$E_x^{III} = \sum_{p,q} D_x^{p,q} \psi_1^{p,q}(x,y)\exp(-ik_z^{p,q}z), \tag{3}$$

$$E_y^{III} = \sum_{p,q} D_y^{p,q} \psi_1^{p,q}(x,y)\exp(-ik_z^{p,q}z), \tag{4}$$

where

$$\psi_1^{m,n}(x,y) = \exp\left[i\left(k_x + \frac{2m\pi}{d}\right)x\right]\exp\left[i\left(k_y + \frac{2n\pi}{d}\right)y\right] \tag{5}$$

and

$$k_z^{m,n} = \sqrt{\left(\frac{\omega}{c}\right)^2 - \left(k_x + \frac{2m\pi}{d}\right)^2 - \left(k_y + \frac{2n\pi}{d}\right)^2}. \tag{6}$$

The diffracted orders are denoted by m and n, the wave vector of the diffracted order by $\boldsymbol{k}$, the period of the array by d, and the field amplitude by $A^{m,n}$. For the vacuum region above the film (region I) there will be an additional term for the incident field.

Within the layer, the electric fields are only present in the cavities, within which they can be described as waveguide modes [Eqs. (5)–(9)],

$$E_x^{II} = \sum_{s,t} [B_x^{s,t}\psi_2(x,y)\exp(iq_z^{s,t}z) + C_x^{s,t}\psi_2(x,y)\exp(-iq_z^{s,t}z)], \tag{7}$$

$$E_y^{II} = \sum_{s,t} [B_y^{s,t}\psi_3(x,y)\exp(iq_z^{s,t}z) + C_y^{s,t}\psi_3(x,y)\exp(-iq_z^{s,t}z)], \tag{8}$$

where

$$\psi_2(x,y) = \cos\left(\frac{s\pi x}{a}\right)\sin\left(\frac{t\pi y}{a}\right), \tag{9}$$

$$\psi_3(x,y) = \sin\left(\frac{s\pi x}{a}\right)\cos\left(\frac{t\pi y}{a}\right), \tag{10}$$

and

$$q_z^{s,t} = \sqrt{\varepsilon_h\left(\frac{\omega}{c}\right)^2 - \left(\frac{s\pi}{a}\right)^2 - \left(\frac{t\pi}{a}\right)^2}. \tag{11}$$

The order of the waveguide modes are denoted by s and t and the associated propagation constant is given by $q_z^{s,t}$, the hole side length by a, and the permittivity within the cavity by ε_h. The field amplitudes are denoted by $B_i^{s,t}$ and $C_i^{s,t}$. Using Maxwell's equations, the magnetic field $\boldsymbol{H}$, can be obtained for all three regions. The tangential boundary conditions require that the electric field must be continuous at each interface across the entire unit cell while the magnetic field must be continuous across the aperture at each interface. Application of these boundary conditions and utilization of the orthogonality condition of the eigenmodes result in pairs of coupled equations in terms of the unknown amplitude coefficients. These equations can be solved to determine an analytical form for the complex transmission and reflection amplitude coefficients,

$$r^{m,n} = \sqrt{(A_x^{m,n})^2 + (A_y^{m,n})^2}, \tag{12}$$

$$t^{p,q} = \sqrt{(D_x^{p,q})^2 + (D_y^{p,q})^2}. \tag{13}$$

A full description of this method is given by Hendry *et al.*[16] and therefore is not repeated here.

This analytical method provides a complete solution by allowing any number of diffracted (propagating or evanescent) and waveguide modes to be included in the calculation. This flexibility allows us to gain an understanding of the influence of specific orders on the structure's overall EM response. Figure 2(a) compares numerical results using the modal matching method (for the first three diffracted orders) with a FEM model[27] for the transmission through a hole array with pitch (d) of 10 mm and hole side (a) of 3 mm illuminated at normal incidence where the incident field vector is polarized along the hole side. At a frequency of ≈29.5 GHz, just below the onset of diffraction, a peak of near-complete transmission is observed despite the system being a well-connected structure (i.e., a structure that perhaps would conventionally be assumed to be a low pass FSS), and the metal filling fraction being 91%. This response is expected as hole array resonances have been well documented as discussed earlier.[9,15,16] Correspondingly, the complementary structure of metal patches (structure A) exhibits enhanced reflection on resonance (not illustrated) despite very low metal occupancy.

Figure 2(b) illustrates the use of Babinet's principle[21] with this method. Babinet's principle has been applied to the transmission results from the hole array to produce the transmission results for the complementary patch array, these are then compared to the full solution produced by a FEM (Ref. 27) model. The agreement is excellent and thus gives confidence in the use of this analytical technique which is far less computationally intensive than full solver, numerical methods. Further, the primary advantage of this technique is that it allows further investigation of the form of the fields and the EM response observed resulting in an improved physical understanding of the response.

Analysis of the resulting equations for the transmission and reflection coefficients shows the dominance of scattering from a particular grating vector, as also reported by Bravo-Abad *et al.*[17] However, further analysis is needed to understand the reason for this dominance. Consider the transmission for structure A* for radiation incident in the *xy* plane; as the structure is two dimensional, it is only necessary to consider the first-order waveguide mode [i.e., $s=1$; $t=0$ for transverse electric (TE) and $s=0$; $t=1$ for transverse magnetic (TM)]. The inclusion of the orders in the calculation is purely as a "matching condition" across the interfaces, and therefore the first-order mode is sufficient to provide an accurate representation of the behavior. Applying these simplifications gives the following general equation for the transmission amplitude coefficient:

$$t^{p,q} = \frac{\frac{\left(\frac{\omega}{c}\right)^2}{\sqrt{\left(\frac{\omega}{c}\right)^2 - (k_x)^2}} (Q^{0,0,s,t})^* \sum_{p,q} Q^{p,q,s,t}}{\sum_{m,n} \left[\frac{(k_z^{m,n})^2 + \left(k_x + \frac{2m\pi}{d}\right)^2}{k_z^{m,n}} \right] (Q^{m,n,s,t})^* Q^{m,n,s,t}}, \tag{14}$$

where

$$Q^{m,n,s,t} = \int_0^a \int_0^a \sin\left(\frac{s\pi y}{a}\right) \cos\left(\frac{t\pi x}{a}\right) \exp\left[-i\left(k_x + \frac{2m\pi}{d}\right)x\right] \exp\left[-i\left(k_y + \frac{2n\pi}{d}\right)y\right] dxdy. \tag{15}$$

The diffracted orders above the film are denoted by m and n, the diffracted orders below the film by p and q, and $Q^{m,n,s,t}$ represent the "overlap integrals" produced by applying the boundary and orthogonality conditions. The observed resonance occurs in the nondiffracting region and therefore only the specular transmission is required (i.e., $p=q=0$). The resulting expression for the transmission is given by

$$t^{0,0} = \frac{\frac{\left(\frac{\omega}{c}\right)^2}{\sqrt{\left(\frac{\omega}{c}\right)^2 - (k_x)^2}} (Q^{0,0,s,t})^* Q^{0,0,s,t}}{\sum_{m,n} \left[\frac{(k_z^{m,n})^2 + \left(k_x + \frac{2m\pi}{d}\right)^2}{k_z^{m,n}} \right] (Q^{m,n,s,t})^* Q^{m,n,s,t}}. \tag{16}$$

Examination of Eq. (16) shows that the transmission reaches a maximum when $\left[\frac{(k_z^{m,n})^2+(k_x+\frac{2m\pi}{d})^2}{k_z^{m,n}}\right]$ is a minimum. By differentiating and substituting the full expression for $k_z^{m,n}$, it can be determined that for $\{m,0\}$ orders this condition occurs when $\frac{\omega}{c} \rightarrow \sqrt{2}(k_x+\frac{2m\pi}{d})$; and for $\{0,n\}$ orders when $\frac{\omega}{c} \approx \sqrt{2[(k_x)^2+2(\frac{n\pi}{d})^2]}$. Further investigation reveals that for incident TE polarization, the $\{m,0\}$ orders dominate the effect, as predicted, due to the associated overlap integrals, Q, also being large under this condition; while for incident TM polarization, the Q terms are large for the $\{0,n\}$ orders. The electric field on the surface of the film in region III is described by

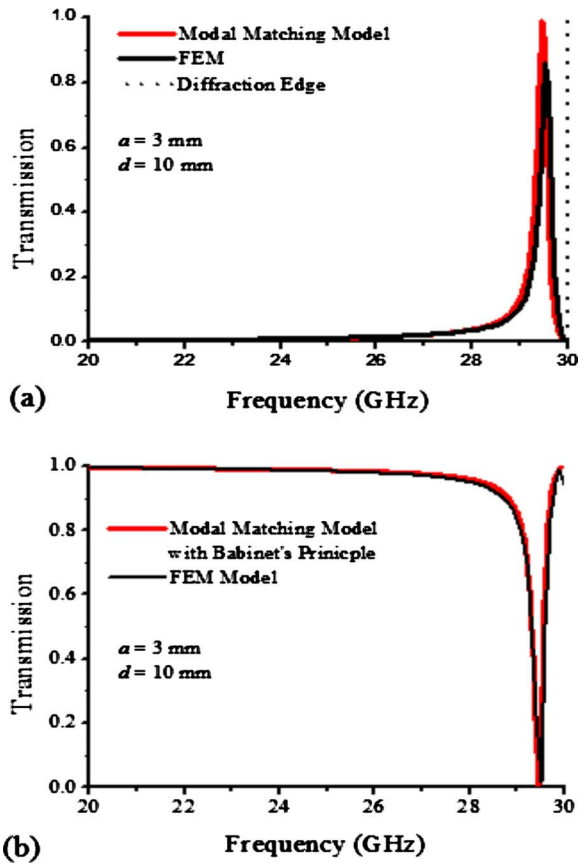

FIG. 2. (Color online) (a) Comparison between modal matching model with third family of evanescent orders in the calculation, compared to a full solution FEM model for structure A* with $a=3$ mm and $d=10$ mm. (b) Comparison between modal matching model data after application of Babinet's principle with a full solution FEM model for structure A with $a=3$ mm and $d=10$ mm.

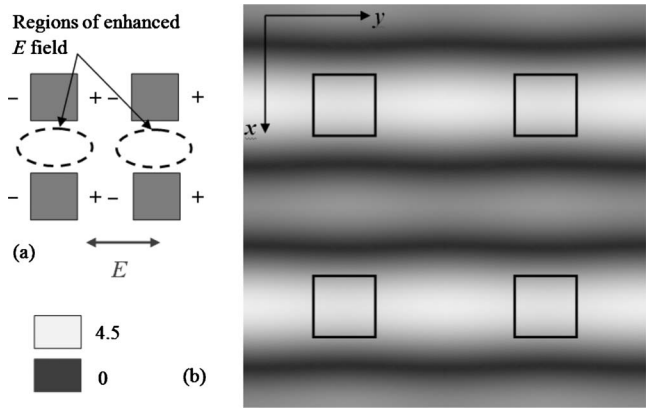

FIG. 3. (a) Schematic of dipole array description showing the regions of enhanced ***E*** field for structure A; (b) ***E*** field plots using a commercial FEM program (Ref. 27) 8 mm below the structure showing the ***E*** field enhancement for structure A with the incident ***E*** field polarized along the y axis illustrating the domination of scattering from the $(0,k_g)$ grating.

$$E^{III} = \sum_{m,n} t^{m,n} \exp\left[i\left(k_x + \frac{2m\pi}{d}\right)x\right]\exp\left[i\left(\frac{2n\pi}{d}\right)y\right]. \tag{17}$$

At the resonant condition for TE polarized radiation, this field is dominated by the $t^{m,0}\exp[i(k_x+\frac{2m\pi}{d})x]$ term. This term describes a surface plane-wave component propagating in the x direction with wave vector $(k_x+\frac{2m\pi}{d})$. Using the same approach, it can be shown that for incident TM polarization, the dominant term is given by $t^{0,n}\exp[i(\frac{2n\pi}{d})y]$ describing a surface plane-wave component propagating in the y direction.

Conversely, for the patch array (structure A), Babinet's principle predicts that it is the TE polarization that will result in a dominant surface plane-wave component propagating in the y direction and the TM polarization is required to produce a dominant component propagating in the x direction. These wave components can be interpreted by considering

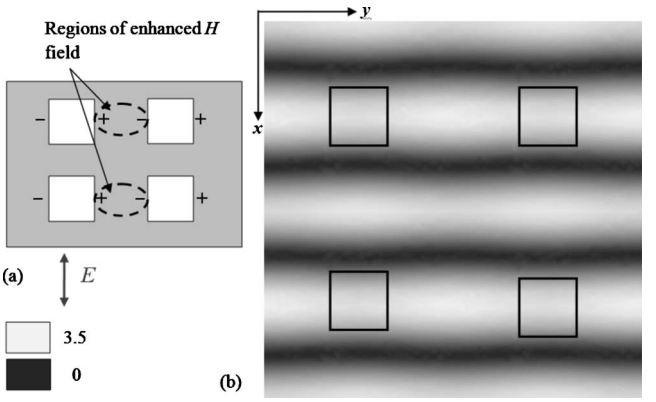

FIG. 4. (a) Schematic of surface current description showing the regions of enhanced ***H*** field for structure A* (b) ***H*** field plots using a commercial FEM program (Ref. 27) 8 mm below the structure showing the ***H*** field enhancement for structure A* with the incident ***E*** field polarized along the x axis illustrating the domination of scattering from the $(m,0)$ grating.

an incident electric field upon the patch array (structure A) that induces a dipolar response in the patches. Each of these dipoles radiate and the strong radiated fields are in a plane orthogonal to the orientation of the dipoles. This dipolar interpretation is well known and has been used to describe the system in the small-patch limit.[25] This leads to regions of enhanced electric (***E***) fields in the spaces between the patches orthogonal to the polarization direction. The resultant large modulation in electric field in this reflects the fact that scattering from the grating vector perpendicular to the polarization dominates the response [Fig. 3(a)]. Figure 3(b) shows the electric field enhancement for structure A, produced using a commercial FEM program,[27] 8 mm below the array. Close to the film, there is strong modulation in both directions (not shown), however, exploring the fields further away shows that the scattering from the grating vector parallel to the incident field, $(m,0)$, decays very quickly with distance, and the scattering from $(0,n)$ dominates.

Dipoles are also induced in the hole array upon application of an electric field; however, these are not discrete dipoles as this is a connected structure and therefore supports

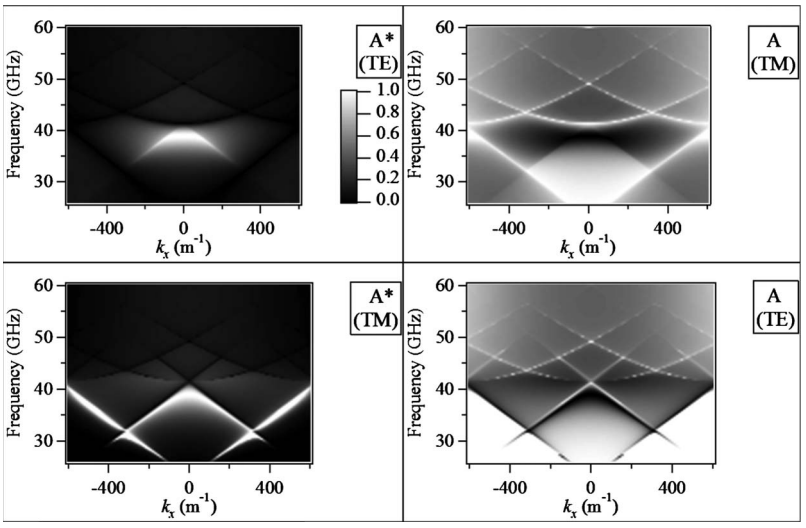

FIG. 5. Dispersion plots using the modal matching model for the transmission for TM and TE polarizations for structures A and A* with $a=6$ mm and $d=10$ mm. The complementary nature of the responses between the two arrays is clearly evident.

real surface currents. These surface currents run parallel to the $\boldsymbol{E}$ field but due to the presence of the holes, there is enhancement of the surface current density at the narrowest point (between the holes). This results in regions of enhanced magnetic ($\boldsymbol{H}$) fields orthogonal to the surface current direction. Similarly to the patch array, it is these regions of enhanced field and the resultant field modulation that leads to the scattering from the grating vector *parallel* to the polarization dominating the response, i.e., $(0,n)$ (Fig. 4).

Babinet's principle describes a complementary relationship between the transmission response of a 2D PEC screen and its inverse. The analytical data (Fig. 5) indicate that for different polarizations in each array, the incident radiation preferentially scatters more strongly from one grating. In the patch array, for TM polarization the mode closely follows the (0, 1) and $(0,-1)$ diffracted light lines while for TE polarization, it follows the $(-1,0)$ and (1, 0) light lines. This is shown in Fig. 5 and the complementary nature is clearly evident in the nondiffracting region below the light line.

This complementary relationship between the observed enhanced responses of hole and patch arrays raises the interesting question as to how the observed response will behave as the fill fraction of a patch array increases to the point at which the system becomes electrically connected. Consider a square array of square PEC patches rotated by 45° about their center in vacuum (structure B) and its inverse (structure B*) [Fig. 6(a)]. This somewhat unconventional geometry results in electrical continuity being established at 50% metal fill fraction unlike for structure A where electrical connectivity does not result until 100% fill fraction. While the response of films as a function of fill fractions has been investigated before,[15] these investigations tend to be on either electrically connected or disconnected systems such as structure A and A*. The self-similarity that results for structures B and B* allows the microwave response of both systems for the entire range of filling fractions to be predicted by only considering filling fractions between 0% and 50% for one of the structures and employing Babinet's principle to predict the response of the complementary structure.

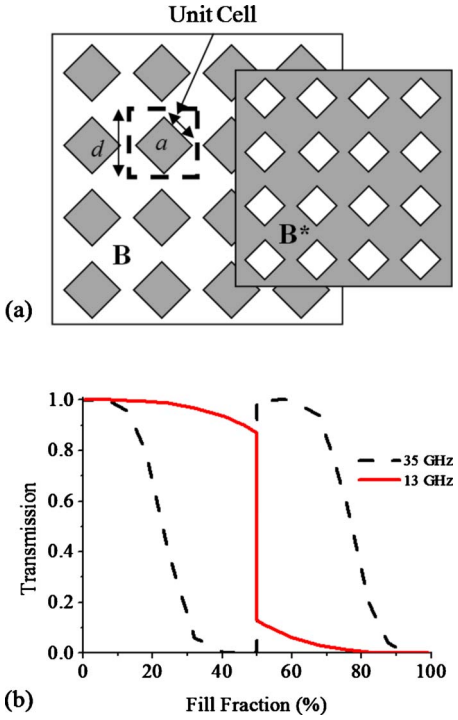

FIG. 6. (Color online) (a) Schematic of the modified structure B and its complementary system B* and (b) transmission through structure B* at normal incidence as a function of metal filling fraction for 13 and 35 GHz.

The modal matching method is now applied to analyze the response of structure B*. Although the electric fields in regions I and III can still be described by a 2D Fourier-Floquet expansion of the diffracted orders of the form described in Eqs. (1) and (2), $\psi_1(x,y)$ now takes the form

$$\psi_1(x,y) = \exp\left[i\frac{2m\pi}{d}\left(\frac{x+y}{\sqrt{2}}\right)\right]\exp(ik_x x)\exp\left[i\frac{2n\pi}{d}\left(\frac{y-x}{\sqrt{2}}\right)\right]\exp(ik_y y). \tag{18}$$

All symbols have the same meaning as defined before. The equations describing the waveguide modes are unchanged; however, care must be taken when applying the orthogonality and boundary conditions to ensure that the boundaries are defined correctly with respect to the rotated hole.

For low frequencies a "step change" from high to low transmission occurs when electrical continuity is established (for structure B this is at 50% occupancy), although as the frequency is increased this step change is expected to be "softened." The 13 GHz data of Fig. 6(b) illustrates this softened response caused by the influence of evanescent diffraction. However, as the frequency becomes more comparable to the onset of propagating diffraction, the strength of the evanescent diffraction is such that the resulting resonance perturbs the response so strongly that the step change is completely reversed as shown by the 35 GHz data of Fig. 6(b).

In conclusion, using a modal matching method, a complete analytical solution for the reflectance and transmission from a thin metal-dielectric film has been derived, showing enhanced reflectance from low metal occupancy structures and enhanced transmission from high metal occupancy structures. The method allows for fast calculations and its flexibility means that successively higher evanescent diffracted and waveguide orders can be included separately, confirming the origin of observed features. As predicted by Babinet's

principle, the response of each structure and its inverse has a complementary relationship. Exploration of the analytical expressions obtained for the transmission through each structure explains the origin of the observed resonances and demonstrates their complementary nature. The importance of the role of the evanescent diffraction has been illustrated, showing that it can perturb the response to such an extent that the expected step change in transmission at electrical connectivity can be completely reversed. The method can be extended to model more complex two- and three-dimensional systems including, but not limited to, arrays incorporating multiaperture unit cells or patches, rotated geometry, and multilayer systems.

M.C.T. would like to thank BAE Systems Ltd. for their financial support and, in particular, Sajad Haq for his continued support. A.P.H. wishes to acknowledge the continued support of the EPSRC.

[1] F. J. García de Abajo, Rev. Mod. Phys. **79**, 1267 (2007).
[2] T. W. Ebbesen, H. J. Lezec, H. F. Ghaemi, T. Thio, and P. A. Wolff, Nature (London) **391**, 667 (1998).
[3] B. A. Munk, *Frequency Selective Surfaces* (Wiley, New York, 2000).
[4] E. L. Pelton and B. A. Munk, IEEE Trans. Antennas Propag. **22**, 799 (1974).
[5] A. A. M. Saleh and R. A. Semplak, IEEE Trans. Antennas Propag. **24**, 780 (1976).
[6] R. J. Kelly, M. J. Lockyear, J. R. Suckling, J. R. Sambles, and C. R. Lawrence, Appl. Phys. Lett. **90**, 223506 (2007).
[7] R. Ulrich, Infrared Phys. **7**, 37 (1967).
[8] J. B. Pendry, Science **306**, 1353 (2004).
[9] F. J. Garcia-Vidal, L. Martin-Moreno, and J. B. Pendry, J. Opt. A, Pure Appl. Opt. **7**, S97 (2005).
[10] L. B. Whitbourn and R. C. Compton, Appl. Opt. **24**, 217 (1985).
[11] R. C. Compton, IEEE Trans. Microwave Theory Tech. **33**, 1083 (1985).
[12] J. H. Coggon, Geophysics **36**, 132 (1971).
[13] L. F. Shen, X. D. Chen, and T. J. Yang, Opt. Express **16**, 3326 (2008).
[14] J. B. Pendry, L. Martin-Moreno, and F. J. Garcia-Vidal, Science **305**, 847 (2004).
[15] J. Bravo-Abad, L. Martin-Moreno, F. J. Garcia-Vidal, E. Hendry, and J. Gomez Rivas, Phys. Rev. B **76**, 241102 (2007).
[16] E. Hendry, A. P. Hibbins, and J. R. Sambles, Phys. Rev. B **78**, 235426 (2008).
[17] J. Bravo-Abad, F. J. Garcia-Vidal, and L. Martin-Moreno, Phys. Rev. Lett. **93**, 227401 (2004).
[18] R. C. Mcphedran, G. H. Derrick, and L. C. Botten, *Electromagnetic Theory of Gratings* (Springer-Verlag, Berlin, 1980).
[19] A. Mary, S. G. Rodrigo, L. Martin-Moreno, and F. J. Garcia-Vidal, Phys. Rev. B **76**, 195414 (2007).
[20] F. J. García de Abajo and J. J. Sáenz, Phys. Rev. Lett. **95**, 233901 (2005).
[21] M. Born and E. Wolff, *Principles of Optics* (Cambridge University Press, Cambridge, 2002).
[22] F. Falcone, T. Lopetegi, M. A. G. Laso, J. D. Baena, J. Bonache, M. Beruete, R. Marques, F. Martin, and M. Sorolla, Phys. Rev. Lett. **93**, 197401 (2004).
[23] O. Luukkonen, C. Simovski, G. Granet, G. Goussetis, D. Lioubtchenko, A. V. Raisanen, and S. A. Tretyakov, IEEE Trans. Antennas Propag. **56**, 1624 (2008).
[24] R. C. Compton, L. B. Whitbourn, and R. C. Mcphedran, Appl. Opt. **23**, 3236 (1984).
[25] F. J. García de Abajo, R. Gómez-Medina, and J. J. Sáenz, Phys. Rev. E **72**, 016608 (2005).
[26] C. Rockstuhl, T. Zentgraf, T. P. Meyrath, H. Giessen, and F. Lederer, Opt. Express **16**, 2080 (2008).
[27] ANSOFT HFSS™, Release 11.2.1.